Available online at www.sciencedirect.com
SCIENCE DIRECT®
Polymer 44 (2003) 3269–3277
polymer
www.elsevier.com/locate/polymer

How does an oxygen atom in the side chain affect the photophysical properties of alkoxy-substituted organopolysilane homopolymers and copolymers?

Haruhisa Kato[a], Takashi Karatsu[a,*], Akira Kaito[b], Shigetomo Matsuyama[b], Akihide Kitamura[a,*]

[a]*Department of Materials Technology, Faculty of Engineering, Chiba University, 1-33 Yayoi-cho, Inage-ku, Chiba 263-8522, Japan*
[b]*National Institute of Advanced Industrial Science and Technology (AIST), 1-1 Higashi, Tsukuba, Ibaragi 305-8565, Japan*

Received 13 December 2002; received in revised form 25 February 2003; accepted 14 March 2003

Abstract

Alkoxy-substituted organopolysilane homopolymer (poly[SiMe(OR)]$_n$) and random copolymers (poly[SiMe(OR)]$_m$[SiMeR′]$_n$ were synthesized and the solvatochromism and thermochromism for their absorption and fluorescence spectra were examined. The band maxima shifted to longer wavelengths with an increase in the ratio of the alkoxy side chains; however, the influence of the solvent was very small. The thermochromic shifts are dependent on the number of alkoxy side chains. Molecular dynamics calculation showed that the conformation of the polysilanes was determined by the Coulomb interaction between the alkoxy side chains, and the conformations of the polyalkoxysilanes are similar to those of polyalkylsilanes (poly[SiRR′]$_n$). Molecular orbital (MO) calculations manifested that the interaction between the orbitals of the oxygen atom in the side chain and those of the silicon atom in main chain (σ conjugation system) was larger in LUMO than in HOMO, and the decrease in LUMO energy shifted the absorption maxima to longer wavelength.

Keywords: Polysilane; Photophysical properties; Alkoxy side chain

1. Introduction

It was known that delocalized σ electrons on the Si–Si bonds of polysilanes produce unique electronic and optical properties, such as electroluminescence, photoconductivity, thermochromism, etc. [1]. The electronic and optical properties of polysilanes have been controlled by introducing various substituents into the silicon backbone [2–10]. The structures of the chiral polysilanes were already studied in detail by light scattering and molecular mechanic calculations, and the various optical properties were observed. The position of the chiral center in the side chain affected the selective spiral conformation of the polysilane, manifest rigidity of main chains of polysilanes occurred due to the bulky side chains. Spectral changes were occurred due to the inversion of their spirals by changing the temperature. Moreover, various trials have also been carried out to control the spectroscopic properties by introducing the substituents containing heteroatoms [11–21]. The polysilanes having oxygen or nitrogen atoms into the side chain have been synthesized recently, and their absorption wavelengths were longer than those of polysilanes having simple alkyl side chains. These polysilanes also showed unique solvatochromism and thermochromism. Interestingly, these two remarkable spectroscopic characteristics were different with the position of the heteroatoms in the side chain. The polysilanes with ether side chains undergo conspicuous spectral changes with change in the solvent or temperature. Poly(dialkoxysilane) has, however, only small thermochromism. In addition, an LB film was easily prepared using the polarity of the side chains and favorable characteristics were observed as optical materials. These new phenomena were caused by the effect of the heteroatoms, but the mechanism of the 'heteroatom effects' is not clear. There are two principal reasons considered. One is the interaction between the heteroatoms in the side chain, for example, steric or electrostatic interaction which affects the conformation of silicon backbone. The other reason is that heteroatoms affect the σ orbital in the Si–Si bonds in

* Corresponding authors. Tel.: +81-43-290-3366; fax: +81-43-290-3039.
E-mail address: karatsu@xtal.tf.chiba-u.ac.jp (T. Karatsu).

0032-3861/03/$ - see front matter © 2003 Elsevier Science Ltd. All rights reserved.
doi:10.1016/S0032-3861(03)00243-X

the main chain. Our recent study on oligosilane with perpentoxy groups showed that the conformation of the silicon backbone gave larger effect on its optical properties further than the interaction between the oxygen non-bonding orbitals and short length of σ conjugation. However, this is not suited for polyalkoxysilanes, because there are many conformations, long or short-range intramolecular interactions, and long length of σ conjugation.

In order to clarify the effects of heteroatoms in the side chains on the photophysical properties of polysilanes, we synthesized polysilanes with *n*-pentoxy substituents, and polysilane copolymers having both pairs of (*n*-pentoxy, methyl) and (hexyl, methyl) substituents. We then measured the absorption and emission spectra of those polysilanes in some solvents. The structures of these polysilanes were analyzed by the multiangle light scattering method, and the intramolecular interactions and the conformation of polysilanes were examined by Molecular dynamics (MD) calculations. We also carried out ab initio MO calculations to understand the orbital interaction between the Si–Si bond and oxygen atoms in the side chains. Combining these experiments and calculations, we estimated the effects of oxygen atoms in the alkoxy side chains on the conformation or optical properties of polyalkoxysilanes.

2. Experimental section

2.1. Sample preparation

Polysilanes and polysilane copolymers with alkoxy side chains were synthesized as shown in Scheme 1. A typical Wurtz coupling reaction was carried out. Sodium (twice as much as the monomer in moles) was stirred in dry toluene and heated at 110 °C under nitrogen atmosphere. Dichlorohexylmethylsilane and dichloromethylphenylsilane, mixed in different proportions, were added to the solution and refluxed for 1 h. The reaction was then stopped by adding 2-propanol. The crude polymers were washed with water, purified by reprecipitation, and dried in a vacuum.

Heteroatom substituted polysilanes were synthesized by

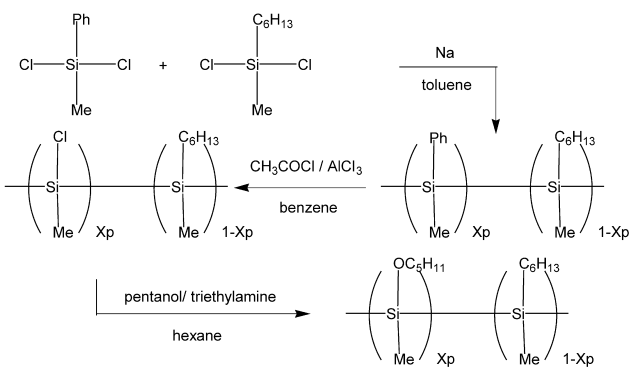

Scheme 1. Synthetic route of alkoxy-substituted polysilane random copolymers.

the method of West et al. [15]. Phenyl-substituted polysilane was dissolved in dry benzene. Aluminum chloride (twice as much as the phenyl in moles) was added to the solution, and acetyl chloride (the same as aluminum chloride in moles) was slowly added to the solution. The solution color changed to dark brown, and stirred for 10-h, then much excess amount of pentanol was poured into the solution, and it was stirred for a day. The crude polymer was dissolved in toluene, washed with water, evaporated, and dried in a vacuum. According to the integration of the ^{1}H NMR spectra, approximately 1 to 5% of the phenyl group remained. However, we assumed that the amount of phenyl groups was too small to affect the optical properties of these polysilanes. The synthesized polysilanes were named as follows. Poly(hexylmethylsilane) and poly(methylpentoxysilane) were named PHMS and PMPOS, respectively. Polysilane copolymers were named HαOβ, where α and β are the ratios of hexyl substituents and pentoxy substituents, respectively. For example, poly(hexylmethylsilane)-*co*-poly(methylpentoxysilane) (1:2) is expressed as H1O2. ^{1}H NMR and ^{29}Si NMR spectra were measured at 600 and 120 MHz, respectively, by a JEOL JNM-LA600 spectrometer as shown in Table 1. $CDCl_3$ was used as the solvent and TMS as the internal standard. The free induction decay signals were accumulated 64–8192 times.

2.2. Size exclusion chromatography–multiangle laser light scattering (SEC–MALLS)

Molecular weight and molecular weight distribution were determined by a Shimadzu LC-6A pump coupled with two Tosoh TSKgel GMH HR-H mixed gel columns at 40 °C (THF, 1.0 ml min^{-1})(Table 1). The columns were calibrated with a series of 14 polystyrene standards of narrow molecular weight distribution (Tosoh Co.). A Tosoh RI 8020 differential refractometer and a Dawn DSP laser photometer (Wyatt Technology Co.) were used as detectors. To detect by the laser photometer, the polymer concentration at each elution time was calculated from the differential refractive index increment (d*n*/d*c*) of the THF solution at 40 °C. The d*n*/d*c* was measured by the differential refractometer using a He–Ne laser, DRM1030 (Photal). The independently determined d*n*/d*c* for the respective polymers were as follows: PHMS:0.217 ml g^{-1}, and H1O3:0.231 ml g^{-1}. The excess Rayleigh ratios were measured at 12 scattering angles in a range of 39 to 139°. After Zimm plots on the respective elution, the molecular weight and radius of gyration were calculated.

2.3. Computational methodology

Ab initio MO calculations were carried out using the GAUSSIAN98 program on IBM-RS/6000-SP. Decahydroxyltetrasilane: (OS4), *meso* and *racemo*-dihydroxyloctamethyltetrasilane (OS4M and OS4R, respectively), and decamethyltetrasilane (MS4) were used as model

Table 1
Characteristics of polysilane homopolymers and copolymers studied in this work

Polymers	M_w^{ps} (g mol^{-1})[a]	^{1}H NMR	^{29}Si NMR	x_p[b]
PMPOS	18800	Me: −0.7 to 0.5, OC_5H_{11} (OCH_2: 3.5–3.8, CH_2: 1.2–15, 1.5–1.8, CH_3: 0.8–1.1)	0.5–9.5	–
PHMS	482000	Me: −0.7 to 0.5, C_6H_{13} (CH_2: 0.9–12, CH_3: 0.8–09)	−35.5 to −29.5	–
H104	32000	Me: −0.7 to 0.5, OC_5H_{11} (OCH_2: 3.5–3.8, CH_2: 1.2–15, 1.5–1.8, CH_3: 0.8–1.1); C_6H_{13} (CH_2: 0.8–1.3, CH_3: 0.7–0.8)	−1.0 to 8.5, −35 to −27	0.8
H103	48200	Me: −0.7 to 0.5, OC_5H_{11} (OCH_2: 3.5–3.8, CH_2: 1.2–1.5, 1.5–1.8, CH_3: 0.8–1.1); C_6H_{13} (CH_2: 0.8–1.3, CH_3: 0.7–0.8)	−1.0 to 8.5, −35 to −27	0.74
H102	28100	Me: −0.7 to 0.5, OC_5H_{11} (OCH_2: 3.5–3.8, CH_2: 1.2–1.5, 1.5–1.8, CH_3: 0.8–1.1); C_6H_{13} (CH_2: 0.8–1.3, CH_3: 0.7–0.8)	−1.0 to 8.5, −35 to −27	0.65
H101	25000	Me: −0.7 to 0.5, OC_5H_{11} (OCH_2: 3.5–3.8, CH_2: 1.2–1.5, 1.5–1.8, CH_3: 0.8–1.1); C_6H_{13} (CH_2: 0.8–1.3, CH_3: 0.7–0.8)	−1.0 to 8.5, −35 to −27	0.47
H201	35000	Me: −0.7 to 0.5, OC_5H_{11} (OCH_2: 3.5–3.8, CH_2: 1.2–1.5, 1.5–1.8, CH_3: 0.8–1.1); C_6H_{13} (CH_2: 0.8–1.3, CH_3: 0.7–0.8)	−1.0 to 8.5, −35 to −27	0.38

[a] M_w^{ps} is obtained by SEC using polystyrene standard.
[b] $x_p = \beta/(\alpha+\beta)$, where α is ratio of hexyl substituents and β is those of pentoxy substituents, calculated by ^{1}H NMR.

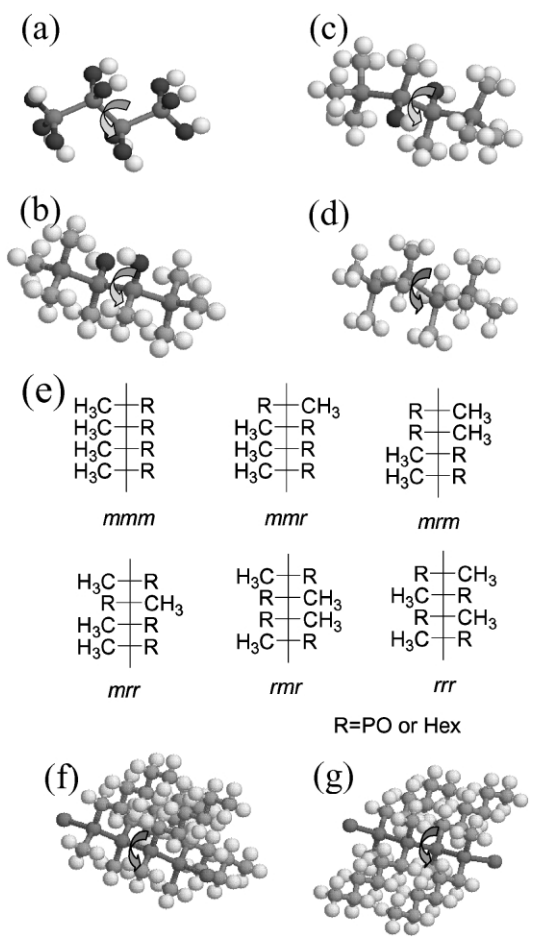

Fig. 1. Schematic representation of calculated model compounds of oligosilanes: (a) OS4, (b) OS4M, (c) OS4R, and (d) MS4. Variable dihedral angles of Si–Si–Si–Si for calculations are indicated in the figures, (e) zigzag projection formula of six tetrad microstructures, (f) simple model of PH (*mmm*), and (g) simple model of PH(*rrr*).

compounds in this study (see Fig. 1a–d), because polysilanes were too large to use in performing ab initio MO calculations. In order to discuss the effects of oxygen atoms on the silicon backbone, the composition of methyl and oxyl groups in the oligosilanes was changed, as shown in these four models. The geometries were fully optimized by the MO calculations at the B3LYP/6-31G** level. The default criteria for convergence were used for all the optimizations. Using the geometries as determined above, CIS calculations were performed at the CIS/6-31G* level. In these calculations, the dihedral angles of the central Si–Si bonds were set at a given dihedral angle, for tetrasilanes at every 10°.

MD calculations were carried out using the PCFF force field, which was optimized by Sun for silicon-backbone compounds [22–25]. All calculations were performed using the general molecular mechanics program Cerius2 (Accelrys, Inc.). In this simulation, long-range non-bonded forces were cut off above 9 Å, and the temperature was stable throughout the data collection periods. For a simplification of the MD calculation, $(Me(Si(PO)_2)_3(SiMePO)_4(Si(PO)_2)_3Me)$, where PO means a pentoxy group, and $(Me(Si(Hex)_2)_3(SiMeHex)_4(Si(Hex)_2)_3$ Me), where Hex means a hexyl group, were used as model compounds (abbreviated PPO and PH, respectively, in this study). The conformation of the central Si–Si bond was then changed to examine the conformational energies. In addition, PPO and PH have tacticity because of the asymmetrical side chain. Considering only one central dihedral angle, there are six tetrad microstructures: *mmm*, *mmr*, *mrm*, *mrr*, *rmr*, and *rrr* (*m*—meso, *r*—racemo), as shown in Fig. 1e. We have illustrated *mmm* and *rrr* in Fig. 1f and g, respectively. For each tetrad microstructure, the calculations of the conformational energies of the silicon backbone were carried out as follows. First, the central Si–Si bonds were set in given dihedral angles at every 10°. In order to determine the initial structure for the MD simulation, the geometric parameters were optimized by

molecular mechanics calculations using the same force field. In the MD calculation, the temperature was initially set at 600 K for 1 ps and then decreased to 298.15 K. After the system was assumed to reach equilibrium, the total energies, recorded for 500 ps at 10 fs intervals, were averaged. The atomic partial charges were calculated at every 10 fs by the QEQ method [26].

3. Results and discussion

3.1. UV absorption and fluorescence emission spectra for polyalkoxysilanes

The UV absorption spectra of the polysilanes and polysilane copolymers in THF are shown in Fig. 2a. In the case of PMPOS, the band maximum was observed at a longer wavelength compared with PHMS, which had a side-chain length similar to that of a pentoxy group. Fig. 2b shows the band maxima for polysilanes as a function of the ratio of alkoxy substituents. This clearly shows that the band maxima were shifted to longer wavelengths by the increase in the ratios of alkoxy substituents. Fig. 3 shows the fluorescence spectra for PMPOS and PHMS in THF. Fluorescence emission maxima were observed at 330 and 365 nm for PHMS and PMPOS, respectively. The Stokes shift is about 30 nm, and another polysilanes have the similar values.

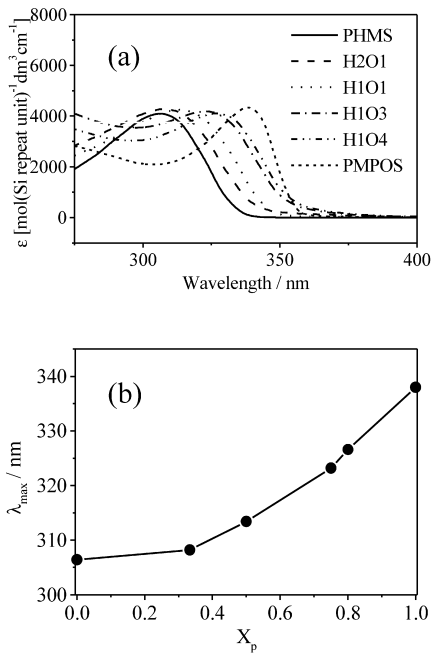

Fig. 2. (a) UV absorption spectra of various polysilanes and polysilane copolymers in THF at room temperature, and (b) UV absorption maxima of various polysilanes in THF at room temperature as a function of the fraction of the pentoxy groups, $x_p = \beta/(\alpha + \beta)$, where α and β are the ratio of hexyl substituents and pentoxy substituents, respectively.

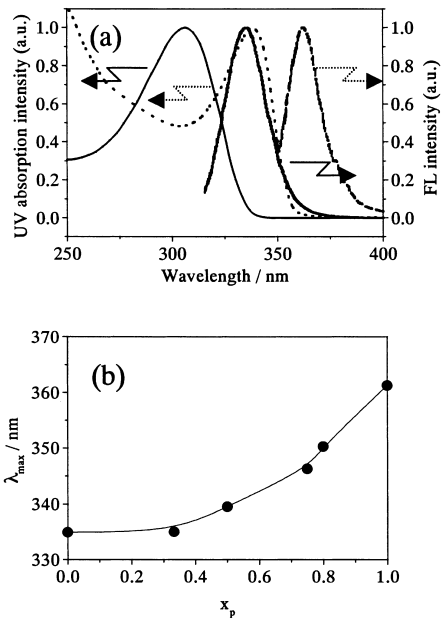

Fig. 3. (a) Fluorescence spectra of PMPOS and PHMS excited at UV absorption maxima in THF at room temperature, and (b) FL band maxima in THF as a function of the fraction of pentoxy groups.

3.2. Conformational analysis of polysilanes

It is well known that the optical properties of polysilanes are largely dependent on their conformation [27–31]. Therefore, we carried out conformational analysis of polyalkoxysilanes. In order to discuss the effects of oxygen atoms on the conformation of the silicon backbone, we compared PPO with PH in Fig. 4. The potential energy

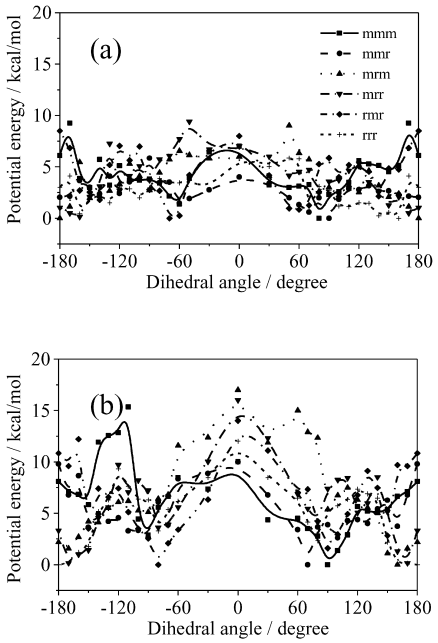

Fig. 4. Calculated ground state potential energies of polysilane model compounds for each tetrad microstructure as a function of the central dihedral angles in the Si-backbone, (a) PH, and (b) PPO.

surfaces as a function of the dihedral angles of the central Si–Si bond for PH and PPO were calculated for six types of possible tetrad microstructures: *mmm*, *mmr*, *mrm*, *mrr*, *rmr*, *rrr*. The potential energy curves for of each model compound have two similar energy minima for *trans* (ca. 150–170°) and *gauche* (ca. 60–90°) conformations.

These polysilane models have two types of energy surfaces. One is the energy surface in which the energy minimum is at the *trans* conformation, matched to *mrm*, *mrr*, and *rrr* tetrad microstructures. The other is the energy surface in which the energy minimum is at the *gauche* conformation, symmetrically. This type is obtained for *mmm*, *mmr*, and *rmr* tetrad microstructures. These tendencies are similar, irrespective of alkyl or alkoxy side chains. The effects of tetrad microstructures on potential energy surface are common for PH and PPO; however, the potential energy differences between the stable and unstable conformations in the respective tetrad microstructures are much larger for PPO than that for PH.

We summarized the calculated potential energies: (*trans* $^{+}$, *trans* $^{-}$, *gauche* $^{+}$, and *gauche* $^{-}$) for six tetrad microstructures in Tables 2 and 3. For instance, such four conformers of *mmm* are shown in Fig. 5. As shown in Tables 2 and 3, most of the differences in calculated potential energies between *trans* and *gauche* conformations are much larger in the polyalkoxysilane models than that in the polyalkylsilane models. These results showed that electrostatic interactions between the oxygen atoms in their side chains are larger than steric interactions between alkyl side chains. These effects might be the origin of the potential energy difference between *trans* and *gauche* conformations; therefore, these are larger in PPO than in PH. It was also estimated that the interaction between long side chains (hexyl and pentoxy, not methyl), which located *gauche* position each other, is the dominant factor determining their conformation in all tetrad microstructures, even if the polysilane has alkyl or alkoxy side chains. For example, in Fig. 5, it was showed that *trans* $^{+}$, *trans* $^{-}$, and *gauche* $^{-}$ conformers have such interaction, while the *gauche* $^{+}$ conformer has no such interaction for *mmm*. Therefore, as shown in Tables 2 and 3, *mmm* takes energy minimum at the *gauche* $^{+}$ conformation.

We also obtained the statistical averaged potential energy surface for each polysilane. To average the potential energies of six tetrad microstructures, we applied Bernoulli's statistics. Previously, polysilanes having asymmetric side chains have been studied by ^{29}Si NMR measurements [32]. In that study, such polysilanes are assumed to take atactic configurations with the same number of *meso* and *racemo* tacticities and that means Bernoulli's statistics could be applied to average the configurations. Then, in this work, we averaged each potential energy surface of each tetrad microstructure, using this assumption. The results for PH and PPO are shown in Fig. 6a and b, respectively. The statistical averaged potential energy surfaces were very similar between the two polysilanes with different side chains, though the energy differences between the *cis* and *trans* conformations are larger in PPO than that in PH. Then, we extracted the Coulomb and van der Waals energies from the potential energy curves. For PPO, the Coulomb energy distribution curve was very similar to that of the potential energy curve, suggesting that the Coulomb repulsion energies are the most important factor on the conformation of polyalkoxysilanes. In addition, the Coulomb interaction between alkoxy side chains makes *cis* conformer more unstable than *trans* conformer for PPO. There are two energy minima at the *trans* and *gauche* conformations in PPO and PH. These two polysilanes are stabilized in the *trans* conformation, and the energy differences between *trans* and *gauche* conformers are almost 0.8 kcal/mol for both PH and PPO. These results mean that these polysilanes are much extended, compared with carbon-backbone polymers. In addition, these polysilanes also seem to take a similar conformation, according to the idea of a rotational isometric state (RIS) model [33], considering only first-order interaction.

We carried out SEC–MALLS measurements on these asymmetric polysilanes. Unfortunately, the molecular weights of most polymers were too low to be able to observe reliable values of the radius of gyration. However, we could measure those for PHMS and H1O3. The results are shown in Fig. 7. These two polysilanes have a similar

Table 2
First-order interaction of potential energies of PH models for each tetrad microstructure (kcal/mol)

	mmm	*mmr*	*mrm*	*mrr*	*rmr*	*rrr*
trans $^{+}$	4.52	2.61	0.00	0.51	2.14	0.00
trans $^{-}$	2.98	2.37	1.97	0.00	1.79	0.44
ganche $^{+}$	0.00	0.00	2.60	2.45	0.84	1.19
gauche $^{-}$	1.37	1.46	2.73	3.73	0.00	2.00

Table 3
First-order interaction of potential energies of PPO models for each tetrad microstructure (kcal/mol)

	mmm	*mmr*	*mrm*	*mrr*	*rmr*	*rrr*
trans $^{+}$	5.05	3.73	0.00	0.16	2.83	0.00
trans $^{-}$	3.82	3.63	0.19	0.00	3.52	0.17
ganche $^{+}$	0.00	0.00	5.36	4.14	1.61	2.25
gauche $^{-}$	2.89	2.63	5.12	3.60	0.00	3.20

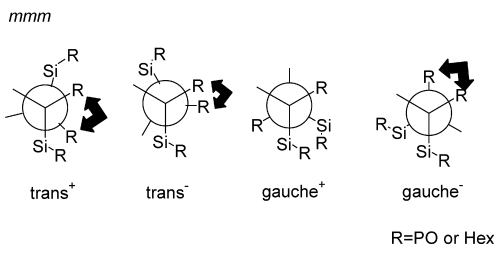

Fig. 5. Newman projection formula of four conformers for *mmm*.

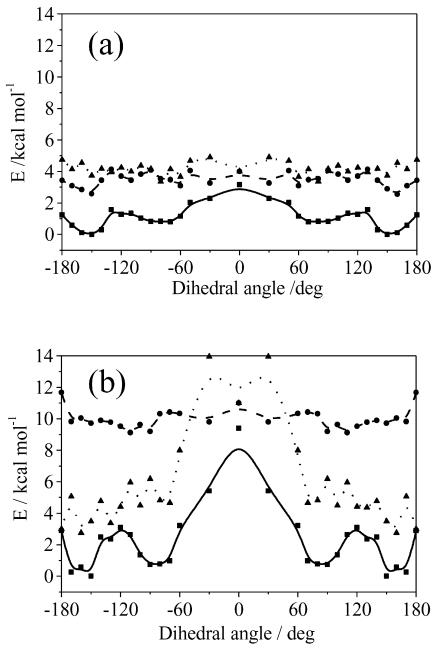

Fig. 6. Averaged conformational energies of polysilane model compounds, (a) PH, and (b) PPO, as a function of central dihedral angles in the Si-backbone, solid line (squares), potential energies; broken line (circles), coulomb energies; dotted line (triangles), van der Waals energies.

radius at the same molecular weight. This result also suggested that these polysilanes have similar global conformations of individual polymer chain in solution, irrespective of alkyl or alkoxy substituents. Under the limitation that MM/MD calculation done here can only estimate local conformation for tetrasilane oligomer model, these results do not contradict each other. The global conformation of polysilane can rationalize from the conformation consist of local conformations calculated for oligomer models.

3.3. Interpretation of optical properties by ab initio MO calculation

From the MD calculations and SEC–MALLS measurements, it was estimated that the conformation of two polysilanes having alkoxy and alkyl side chains are similar. However, as shown in Fig. 2, remarkable effects of oxygen

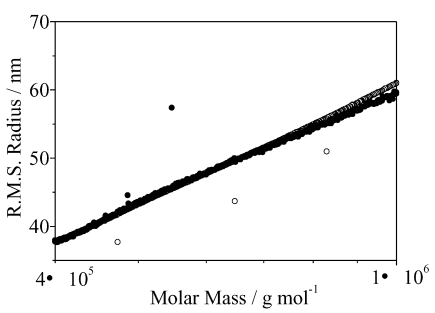

Fig. 7. Radius of gyration of polysilanes as a function of molecular weight: filled circles, PHMS; circles, H1O3.

on the absorption maxima of the polyalkoxysilanes were observed. These results suggest that the conformational effect on spectroscopic properties of polyalkoxysilane is small and characteristic spectroscopic results may be caused by the orbital interaction between the oxygen atom and the Si–Si orbitals. Then, we examined the effects of the orbital of oxygen on the σ-orbital of Si–Si linkage, using tetrasilane models.

Fig. 8a and b shows the results of CIS/6-31G* calculations of singlet excitation energies and the corresponding oscillator strengths as a function of dihedral angles, ϕ_1 for OS4M (see Fig. 1b). Because of a large number of excited states, the results of the four lowest excited states are shown in these figures. Four states are called A and B due to the symmetry of the excited orbital and are numbered from the low-lying excited singlet states. As seen in Fig. 8b, the oscillator strengths of the transitional states of 1B and 2B are calculated to be much stronger than 1A and 2A. The two transitions of 1B and 2B are largely

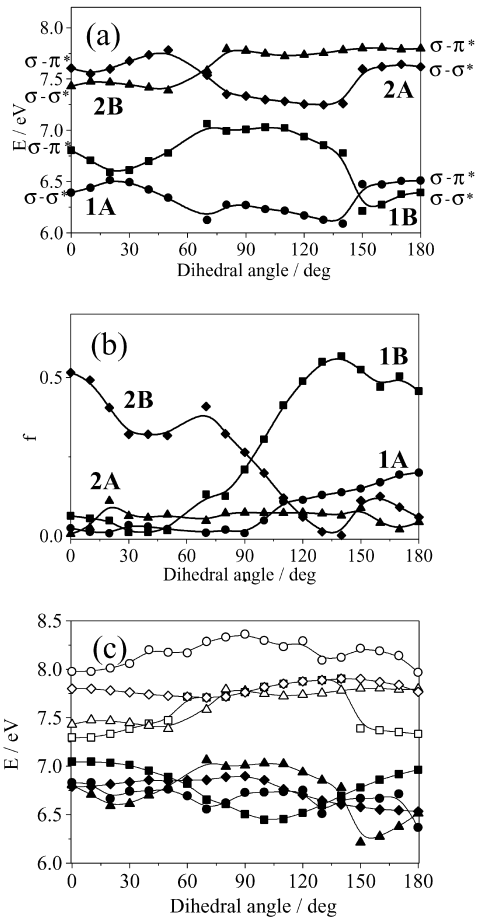

Fig. 8. (a) Calculated (CIS/6-31G*) singlet excitation energies as a function of dihedral angles, and (b) the corresponding oscillator strengths for OS4M: circles, 1A; squares, 1B; triangles, 2A; rhombuses, 2B. (c) Calculated (CIS/6-31G*) singlet excitation energies of 1B and 2B states for oligosilane models as a function of dihedral angles; filled circles, MS4 (1B); circles, MS4 (2B); filled squares, OS4R (1B); squares, OS4R (2B); filled triangles, OS4M (1B); triangles, OS4M (2B); filled rhombuses, OS4 (1B); rhombuses, OS4 (2B) (see in text).

dependent on the dihedral angles, and they have large oscillator strengths in the *trans* and *cis* conformations, respectively. The oscillator strengths of 1B and 2B are crossed near 90°.

We have also carried out ab initio MO calculations for the equal basis sets for other tetrasilane model compounds which have different numbers of alkoxy side chains, in order to clarify the effects of the alkoxy side chains on the Si–Si orbital. We summarized the calculated results of singlet excitation energies as a function of the dihedral angles of these model compounds in Fig. 8c. For the 2B transition, the singlet excitation energies of each model having oxyl side chains are smaller values over all ranges of dihedral angles than that of MS4. Then, it could be estimated that the effects of oxygen on the σ orbital of the Si-skeleton are much larger in a twisted conformation than that in an extended conformation, because the oscillator strength of the 2B transition is larger at the twisted conformation than that at the extended conformation as shown in Fig. 8b. On the other hand, the tendencies of excitation energy distribution for 1B were different with the side chain. The 1B energies of tetrasilanes having asymmetric side chains were largely dependent on the dihedral angles, and they were from 6.5 to 7.0 eV.

Considering the molecular orbital in these tetrasilanes, for MS4, the HOMO consisted of silicon and a connected carbon orbital, and the LUMO consisted of vacant silicon and carbon orbitals. On the other hand, for OS4, the HOMO was constructed of orbitals of oxygen and silicon, and the LUMO was constructed of vacant oxygen and silicon orbitals. In addition, for the polysilane copolymer models; OS4M and OS4R, the HOMO was composed of oxygen, silicon, and carbon orbitals; however, the LUMO was mainly constructed of oxygen and silicon vacant orbitals. The molecular orbital coefficients of oxygen are larger than that of carbon in all model compounds, and this means that the oxygen orbital largely affects the excited state of Si-backbone compounds. These effects are much larger in the LUMO; therefore, the singlet excitation energies become lower in tetrasilane models with alkoxy side chains than that in MS4. In addition, such effects of oxygen are much larger in a twisted conformation of the silicon backbone than in an extended conformation. Therefore, because a twisted conformation certainly exists in a random coil of polysilanes, polyalkoxysilanes show long wavelength maxima in their absorption spectra.

3.4. Effects of the oxygen atoms on thermochromic and solvatochromic properties

Fig. 9a shows that the solvent effects on the band maxima for polysilanes as a function of the ratio of alkoxy substituents. The band maxima shifted to a longer wavelength due to the increase in alkoxy substituents in all solvents. The shifts of the band maxima are observed for all solvents studied, although the polarities of the solvents

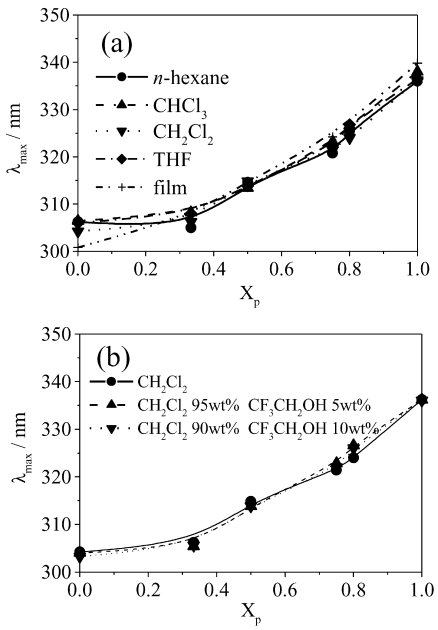

Fig. 9. (a) UV absorption maxima of various polysilanes and polysilane copolymers in various solvents at room temperature as a function of the fraction of pentoxy groups (X_p), and (b) UV absorption maxima for polysilanes and polysilane copolymers as a function of the fraction of X_p in mixed solvents (CH_2Cl_2/CF_3CH_2OH) at room temperature.

are different. In addition, all polysilanes show almost the same maxima in all solvents.

Fig. 9b shows that the band maxima for polysilanes and polysilane copolymers as a function of the ratio of alkoxy substituents in a mixed solvent (CH_2Cl_2/CF_3CH_2OH). The composition of the mixed solvent was changed from 0 to 10 wt% content CF_3CH_2OH in CH_2Cl_2. It was observed that the band maximum was slightly shifted to a shorter wavelength with the increasing ratio of CF_3CH_2OH. These results are similar to those in Fig. 2. Even if the polarity or acidity of the solvent is changed, it is estimated that the spectral change is small. It was already reported that the polysilanes with ether side chains have an obvious solvatochromism in such system. The solvatochromism of such polysilanes was caused by the hydrogen bond between oxygen in the side chain and hydrogen of the solvents [12, 14]. However, polysilanes in this study showed only a small solvatochromism, and this result may be explained by the long carbon side chains, which prevent the approach of the solvents to an oxygen atom in the side chains.

Fig. 10a–c shows the absorption band maxima of polysilanes as a function of temperature. The measurements were carried out in three solvents, which have different polarities ((a) THF, ε 7.52 D, (b) $CHCl_3$, ε 4.81 D, (c) hexane, ε 1.89 D) [34]. When the polysilanes have the same side chains, the tendencies of the shift of band maxima as a function of temperature are very similar for all solvents examined here. In contrast, thermochromism greatly depended upon their side chains. A thermochromic shift of the band maxima for PHMS was much larger than that of

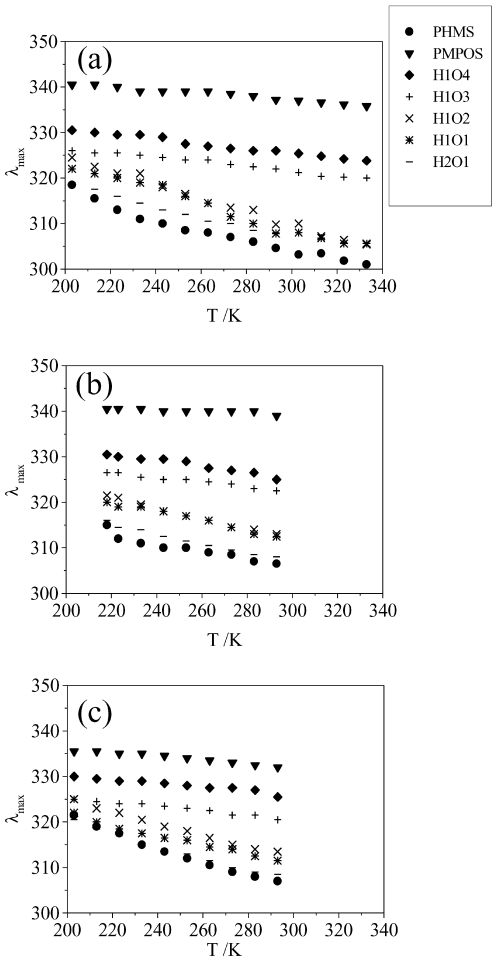

Fig. 10. UV absorption maxima of various polysilanes and polysilane copolymers as a function of temperature (a) in THF, (b) in $CHCl_3$, and (c) in hexane.

PMPOS. The shifts of band maxima became larger with a decreasing ratio of the pentoxy side chains. The solvent effects on the thermochromic shifts of band maxima were different due to the side chains. Thermochromic shifts for the polysilanes with higher ratio of alkyl side chains were larger in non-polar solvent, such as hexane, but the reverse is true in a polar solvent. On the other hand, the thermochromic shifts of polysilanes with higher ratio of alkoxy side chains were larger in polar solvent than that in non-polar solvent.

The thermochromic properties of general polysilanes have unique features, and this is explained by two mechanisms. One is a change in conformation for an isolated polysilane chain [35–42], and the other is aggregation caused by intermolecular or intramolecular side-chain interaction [43–45]. However, the latter mechanism seemed to affect slightly because the concentration of the measurement solution is sufficiently small and it was proved that the silicon backbone moved earlier than the side chain in thermochromism system [41]. Based on the former mechanism, Schweizer proposed that thermochromism was dependent only on a conformational change caused by the interaction between delocalized electrons in the silicon backbone and surrounding molecules such as a side chain or solvents [39,40]. Two factors must be taken into consideration in this theory. One is polarized interaction between the solvents or a side chain and electrons delocalized along the all-*trans* backbone. If this interaction was large, it was predicted that a larger thermochromic system was observed in that theory. The other is the energy difference between an all-*trans* conformation and defective conformation, which disturbed the σ electron delocalization. If this energy difference is large, the thermochromic properties should be weak. Based on this theory, we estimated the thermochromic properties of these polymers.

Considering the polarized interaction, it was predicted that a polyalkoxysilane has a larger interaction with the solvents than a polyalkylsilane, because polarizabilities and ionization energies are much larger for the alkoxy side chain than that for the alkyl side chain. This predicted that the polyalkoxysilanes have a larger thermochromic system than polyalkylsilanes. However, as shown in Fig. 10, there are only small effects due to the polarizabilities of the solvents, because the interaction between the polysilane and the solvents is small, even though the conformational effects on the polarized interaction is expected to be large according to Welsh's study [37]. Unusual σ electron delocalization due to the alkoxy side chains makes it difficult to explain these phenomena.

On the other hand, another mechanism, the energy difference between a *trans* and a defective conformation can easily explain this thermochromism. As shown in Figs. 4 and 5, the energy differences are much larger in a polyalkoxysilane than in a polyalkylsilane. We estimated that this characteristic is caused by the interactions between vicinal alkoxy side chains. According to this assumption, if the numbers of alkoxy side chains decreases, the electrostatic interactions between vicinal alkoxy side chains becomes small and the energy difference becomes small. As shown in Fig. 10, the thermochromic shifts strongly depend on the ratios of the alkoxy side chains. The shifts became larger with a decreasing ratio of alkoxy side chains. Therefore, the thermochromic properties of polysilanes having alkoxy side chains, are reasonably explained by energy difference between an all-*trans* conformation and a defective conformation.

4. Concluding remarks

The absorption maxima of polysilanes having alkoxy side chains shifted to a longer wavelength than that of polysilanes having alkyl side chains, and the shift was proportional to the number of alkoxy side chains. This is explained by the decrease in LUMO energy, which is caused by interaction between oxygen and the Si–Si σ orbital. The conformational interaction was also estimated by MD calculations, and the conformation of polyalkoxysilanes

was determined by the Coulomb interaction between alkoxy side chains. However, the stable conformation of polysilanes is similar to each other, irrespective of alkyl or alkoxy side chain. This was supported by SEC–MALLS measurements. The MO and MD calculations showed that the conformational effects are small on the spectroscopic properties and that orbital interaction between oxygen and silicon atoms affects the optical properties of polyalkoxysilanes. A small solvatochromism was observed, and this is due to the steric hindrance preventing the approach of the solvent to the oxygen atoms. The thermochromic properties of these polysilanes are proportional to the number of the alkoxy side chains. Polysilanes with higher ratios of alkoxy side chains showed a small thermochromism. This is explained by the large difference in conformational energies between an all-*trans* conformation and a defective conformation, which are caused by interaction between oxygen atoms in the side chains.

Acknowledgements

We are grateful to Dr Shinichi Kinugasa, National Institute of Advanced Industrial Science and Technology, for his kind help in the measurement of SEC or SEC–MALLS and for many helpful discussions. This work was supported by a Grant-in-Aid for Scientific Research on Priority Areas (417, No. 14050022) and Scientific Research (No. 14550786) from the Ministry of Education, Culture, Sports, Science and Technology (MEXT) of Japanese Government to T.K.

References

[1] Miller RD, Michl J. Chem Rev 1989;89:1135.
[2] Koe JR, Fujiki M, Motonaga M, Nakashima H. Macromolecules 2001;34:1082.
[3] Nakashima H, Fujiki M. Macromolecules 2001;34:7558.
[4] Natsume T, Wu L, Sato T, Terao K, Teramoto A, Fujiki M. Macromolecules 2001;34:7899.
[5] Toyoda S, Fujiki M. Macromolecules 2001;34:640.
[6] Tachibana H, Kishida H, Tokura Y. Langmuir 2001;17:437.
[7] Fujiki M. J Am Chem Soc 2000;122:3336.
[8] Fujiki M, Motonaga M, Tang H, Torimitsu K, Zhang Z, Koe JR, Watanabe J, Terao K, Sato T, Teramoto A. Chem Lett 2001;30:1218.
[9] Fujiki M, Koe JR, Motonaga M, Nakashima H, Terao T, Teramoto A. J Am Chem Soc 2001;123:6253.
[10] Terao K, Terao Y, Teramoto A, Nakamura N, Fujiki M, Sato T. Macromolecules 2001;34:4519.
[11] Koe JR, Motonaga M, Fujiki M, West R. Macromolecules 2001;34:706.
[12] Oka K, Fujiue N, Nakanishi S, Takata T, West R, Dohmaru T. J Organomet Chem 2000;611:45.
[13] Hsiao Y, Waymouth RM. J Am Chem Soc 1994;116:9779.
[14] Oka K, Fujiue N, Dohmaru T, Yuan C, West R. J Am Chem Soc 1997;119:4074.
[15] Herzog U, West R. Macromolecules 1999;32:2211.
[16] Schwegler LA, Möller M. Acta Polym 1997;48:319.
[17] Seki T, Tohnai A, Tanigaki N, Yase K, Tamaki T, Kaito A. Macromolecules 1997;30:1768.
[18] Nakashima H, Fujiki M. Macromolecules 2001;34:7558.
[19] Seki S, Kunimi Y, Nishida K, Aramaki K, Tagawa S. J Organomet Chem 2000;611:64.
[20] Endo T, Sugimoto Y, Takeda K, Shiraishi K. Synth Met 1999;98:161.
[21] Fukushima M, Tabei E, Aramata M, Hamada Y, Mori S, Yamamoto Y. Synth Met 1998;96:239.
[22] Sun H, Mumby SJ, Maple JR, Hagler AT. J Am Chem Soc 1994;116:2978.
[23] Sun H, Mumby SJ, Maple JR, Hagler AT. J Phys Chem 1995;99:5873.
[24] Sun H. Macromolecules 1995;28:701.
[25] Sun H. Macromolecules 1994;26:5924.
[26] Rappe AK, Goddard WA. J Phys Chem 1991;95:3358.
[27] Klemann BM, West R, Koutsky JA. Macromolecules 1993;26:1042.
[28] Jambe B, Jones A, Devaux J. J Polym Sci, Polym Phys 1997;35:1533.
[29] Klemann BM, West R, Koutsky JM. Macromolecules 1996;29:198.
[30] Kishida H, Tachibana H, Sakurai K, Matsumoto M, Tokura Y. Phys Rev B 1996;54:R14254.
[31] Crespo R, Piqueras MC, Tomas FJ. Chem Phys 1994;100:6953.
[32] Schilling FC, Bovey FA, Zeigler JM. Macromolecules 1986;19:2309.
[33] Mattice WL, Suter UW. Conformational theory of large molecules: the rotational isomeric state model in macromolecular systems. New York, NY: Wiley-Interscience; 1994.
[34] Riddick J, Bunger WB, Sakano TK. Organic solvents: physical properties and methods of purification, 4th ed. New York, NY: Wiley-Interscience; 1986.
[35] Sanji T, Sakamoto K, Sakurai H, Ono K. Macromolecules 1999;32:3788.
[36] Walsh CA, Schilling FC, Lovinger AJ, Davis DD, Bovey FA, Zeigler JM. Macromolecules 1990;23:1742.
[37] Gahimer T, Welsh WJ. Polymer 1996;37:1815.
[38] Yuan C, West R. Macromolecules 1994;27:629.
[39] Sweizer KS. J Chem Phys 1986;85:1156.
[40] Sweizer KS. J Chem Phys 1986;85:1176.
[41] Radhakrishnan J, Kaito A, Tanigaki N, Tanabe Y. Polymer 1999;40:6199.
[42] Kamata N, Aihara S, Ishizaki W, Umeda W, Terunuma D, Yamada K, Furukawa S. J Non-Cryst Solids 1998;227:538.
[43] Shukla P, Cotts PM, Miller RD, Russell TP, Smith BA, Wallraff GM, Baier M. Macromolecules 1991;24:5606.
[44] Miller RD, Wallraff GM, Baier M, Thompson D, De Schryver FC, Declercq D. Polym Prep 1991;32(1):437.
[45] Wallraff GM, Baier M, Miller RD, Rabolt JF, Hallmark V, Cotts PM, Shukla P. Polym Prep 1989;30(2):245.